Controlling chaos of the Ricker population model

Guo Feng[1]

[1]School of Data and Computer Science, Shandong Women's University, Jinan, China 250300

Email: sdwugf@163.com

Abstract: For certain parameters, a class of density dependent Leslie population model has a chaotic attractor. The chaotic dynamics of the Ricker mapping is studied. Control parameter is perturbed slightly depending times by the improvement of OGY. By the pole placement technique of the linear control theory, when the mapping point wanders to the neighborhood of the periodic point, the control parameter is perturbed. The chaotic motion are controlled on the stable periodic period-1 point and period-2 orbits, and the influence of different control parameter ranges on the control average time is analyzed. When the selected regulator poles are different, the number of iterations used to control chaotic motion on a stable periodic orbit is difference. Numerical simulations are presented to illustrate our results with the theoretical analysis and show the effect of the control method. The analysis and results in this paper are interesting in mathematics and biology.

Key words: Ricker mapping; strange attractor; chaos control; pole placement technique

1. Introduction

The Leslie model (Caswell, 2001) is the principal age structured discrete population model, and is commonly used in demography and conservation ecology. Following ecologists' discoveries and in order to help ecologists model such populations, scientific researchers have begun studying extensions of the ubiquitous age structured Leslie population model that allow some survival probabilities and fertility rates to depend on population densities. These nonlinear extensions commonly exhibit very complicated dynamical behavior. Ugarcovici and Weiss (2004) studied Ricker model. This model is described by the two dimensional mapping $R_{a,b} : \mathbb{R}_+^2 \to \mathbb{R}_+^2$

$$R_{a,b}(x,y) = \left((ax + \gamma ay) e^{-\lambda(x+y)}, bx \right) \tag{1}$$

Where x and y stand for the density of the first age group and the second age group. a and γa are the group's initial fertility rates ($a, \gamma > 0$), b is the survival rate from the first age group to the second one and λ is the decay index, $\lambda > 0$. In Eq. (1), the fertility rate monotonically decreases as a function of the total population size, the fertility decay is exponential. Ugarcovici and Weiss (2007) proved that for some parameter regions, Eq,(1) admits a strange attractor which supports a unique physical probability measure.

The study of chaos control began in the late 1980s. The early research idea is to use the existing dynamic control strategies and destroy the conditions for the occurrence of chaotic

motion. Ott, Grebogi and Yorke (1990) proposed a method to control chaos, which is based on the dense embedding of infinite unstable periodic motion in strange attractors, and the various states of chaotic dynamics are close to these unstable periodic movements. Since then, many scholars have put forward different improvement measures according to various situations, and further developed the OGY method, which has laid a good foundation for the application of chaos [6-9]. It has shown that an energy-based feedback controller is capable of changing a chaotic dynamic to other chaotic dynamics [10]. The parameters of a modified Autonomous Van der Pol-Duffing (ADVP) circuit is controlled using linear feedback control [11]. Chaos in a memristor based circuit and nonlinear circuits are controlled using the method of linear feedback control [12-16]. The chaos control of two degree of freedom collision vibration system is studied by OGY method [17].

How to control the chaos of high periodic states and high dimensional dynamic systems in strange attractors is the direction of further improvement of OGY method. Ott, Grebogi, Romeiras and Dayawansa [18] adopt the pole assignment technique in system control to further improve the OGY method.

The chaotic dynamics of the Ricker mapping and the chaos is controlled. The unstable period-1point and unstable period-2 points are controlled on the periodic orbits, and the influence of different control parameter ranges on the control average time is analyzed. In biology or ecology, the complex chaotic behavior of this mapping shows the relationship between the number, birth rate and survival rate in a population, whether it survives in a balanced state or makes the population develop in disorder or chaos. This research can provide theoretical basis and help for the research in biology or ecology.

2. The Leslie model

2.1. The linear Leslie model

Leslie (1945, 1948) introduced the following age-structured linear population model. Consider a population divided into d age-classes or generations, which we call generations 1, 2,...,d. Let $n_k(t)$ be the number of individuals in the kth age-class at time t, measured in generations. The individuals in generations 2,...,d are survivors of the previous generation at time t, and thus one assumes that for 2, 3,...,d.

$$n_k(t+1) = p_{k-1}n_{k-1}(t) \tag{2}$$

where p_i, $i = 1,..., p_{d-1}$ is the probability that an individual of age-class i survives for one generation. The new members of age-class 1 cannot be survivors of any other age-class; they must have originated from reproduction. Thus, Leslie assumed

$$n_1(t+1) = f_1 n_1(t) + f_2 n_2(t) + \cdots + f_d n_d(t) \tag{3}$$

where f_i is the *per* capital fertility of generation i. Hence

$$\begin{pmatrix} n_1 \\ n_2 \\ \vdots \\ n_d \end{pmatrix}(t+1) = \begin{pmatrix} f_1 & f_2 & \cdots & f_{d-1} & f_d \\ p_1 & 0 & \cdots & 0 & 0 \\ \vdots & \vdots & \cdots & \vdots & \vdots \\ 0 & 0 & \cdots & p_{d-1} & 0 \end{pmatrix} \begin{pmatrix} n_1 \\ n_2 \\ \vdots \\ n_d \end{pmatrix}(t) \tag{4}$$

or more compactly,

$$n(t + 1) = An(t)$$

This special age-classified matrix A is called the Leslie matrix. The matrix A is non-negative with positive entries only in the first row and the subdiagonal. Population biologists and demographers use life table analysis to construct the matrix A.

Most Leslie models used for actual demographic forecasting use 5-year age groups instead of three generations, in which case the matrix A becomes a 10×10 matrix. The text Matrix Population Models' by Caswell [1] contains a comprehensive treatment of Leslie model.

2.2. The nonlinear Leslie model

We now consider the Leslie population model where the fertility rates decay exponentially with population size (Ricker-type nonlinearity). In this case, the Leslie matrix A becomes the population-size dependent matrix

$$\mathbf{A}(N) = \begin{pmatrix} f_1 e^{-\lambda N} & f_2 e^{-\lambda N} & \cdots & f_{d-1} e^{-\lambda N} & f_d e^{-\lambda N} \\ p_1 & 0 & \cdots & 0 & 0 \\ \vdots & \vdots & \cdots & \vdots & \vdots \\ 0 & 0 & \cdots & p_{d-1} & 0 \end{pmatrix} \tag{5}$$

One obtains the following system of d nonlinear equations

$$n_1(t+1) = \left(f_1 n_1(t) + f_2 n_2(t) + \cdots + f_d n_d(t) \right) e^{-\lambda \left(n_1(t) + n_2(t) + \ldots n_d(t) \right)}$$

$$n_2(t+1) = p_1 n_1(t)$$

$$\ldots \ldots$$

$$n_d(t+1) = p_{d-1} n_{d-1}(t) \tag{6}$$

3

The associated 2d-parameter nonlinear dynamical system $T: R_d \rightarrow R_d$ is

$$T\begin{pmatrix} x_1 \\ x_2 \\ \vdots \\ x_d \end{pmatrix} = \begin{pmatrix} \left(f_1 n_1(t) + f_2 n_2(t) + \cdots + f_d n_d(t)\right) e^{-\lambda(n_1(t) + n_2(t) + \ldots n_d(t))} \\ p_1 x_1 \\ \vdots \\ p_{d-1} x_{d-1} \end{pmatrix} \tag{7}$$

Note that when $\lambda = 0$, this model reduces to the classical Leslie matrix model. For two and three generations, the corresponding systems are

$$T(x, y) = \left(\left(f_1 x + f_2 y\right) e^{-\lambda(x+y)}, p_1 x\right) \tag{8}$$

and

$$T(x, y, z) = \left(\left(f_1 x + f_2 y + f_3 z\right) e^{-\lambda(x+y+z)}, p_1 x, p_2 y\right) \tag{9}$$

3. The dynamic behavior of the two-generation Ricker type model

The Ricker-type recruitment population model is described by the two dimensional mapping $R_{a,b}: \mathbb{R}_+^2 \rightarrow \mathbb{R}_+^2$

$$R_{a,b}(x, y): \begin{cases} f(x, y) = (ax + \gamma ay) e^{-\lambda(x+y)} \\ g(x, y) = bx \end{cases} \tag{10}$$

Where x and y stand for the density of the first age group and the second one. a and γa are the fertility rates of the group at time zero, b is the survival rate from the first age group to the second one, and λ is the decay index, $\lambda > 0$. For the parameters $\gamma = 0.2, \lambda = 0.1$, and fixed survival rate $b = 0.2$. When the initial fertility rate a changes from 60-90, the dynamic behavior of the Ricker mapping exhibits complicated dynamical behavior. The bifurcation diagrams of Ricker mapping is shown in Figure 1 (a-d).

This type of bifurcation cannot occur for one-dimensional mappings. We now discuss the salient features of the bifurcation diagram. We remark that since this is mainly a numerical study, all bifurcation values are approximate. For $0 < a < 0.455$, $(0, 0)$ is a global attractor. There exists a positive fixed point (equilibrium solution) that is stable for $0.455 < a < 17.5$. (as shown in Figure 1 b). At $a=17.5$, there is a period-2 saddle-node bifurcation that produces an attracting period-2 orbits and its associated period-2 (unstable) saddle orbit. At $a=34.5$, the stable fixed point undergoes a doubling bifurcation (as shown in Figure 1 c). For $34.5 < a < 90$ (as shown in Figure 1

d), where there exist two different transitive attractors, each with a large basin of attraction. At *a*= 85, a Henon-like strange attractor coexists with an attracting invariant curve. This invariant closed curve bifurcates into a strange attractor. The phase diagrams of the mapping when *a* takes different values are consistent with the analysis of the above bifurcation diagrams (as shown in Figure 2).
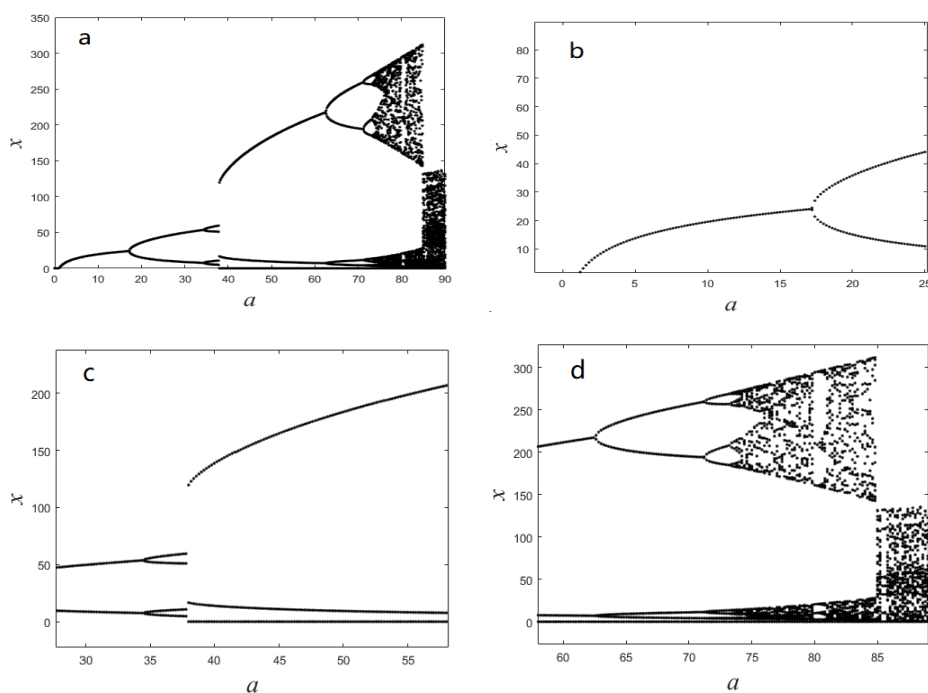

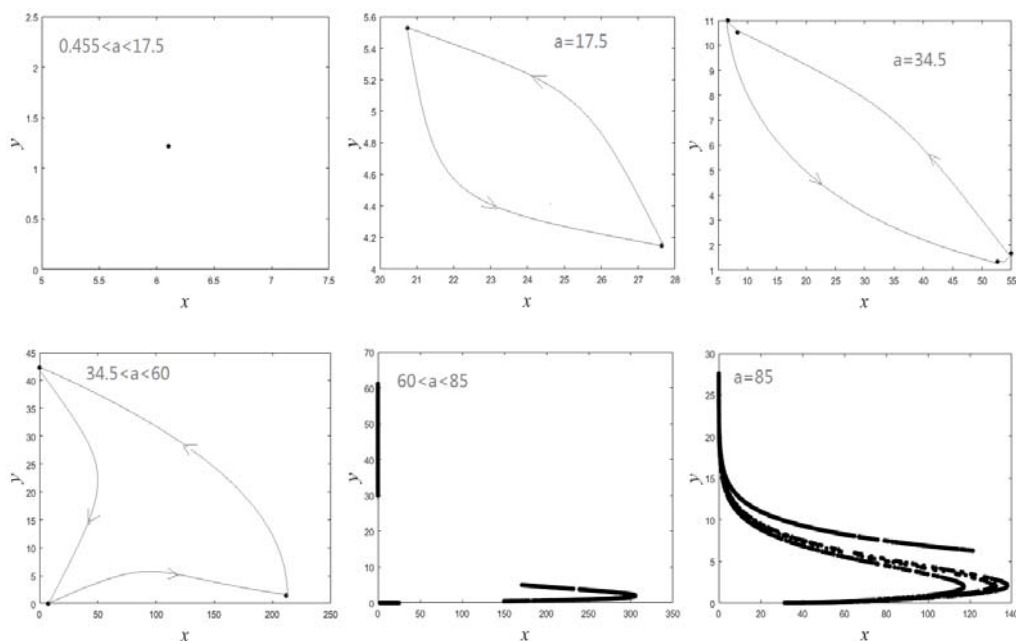Figure 1: Bifurcation diagrams of Ricker mapping (a-d) ($\gamma = 0.2, \lambda = 0.1, b = 0.2$, 0<a<90).

Figure 2: The phase diagrams of Ricker mapping (0<*a*<0.455, 0.455<*a*<17.5,

$a=17.5$, $a=34.5$, $34.5<a<60$, $60<a<85$, $a=85$).

The largest Lyapunov exponent, which has proven to be the most useful dynamic diagnostic tool for chaotic systems, is considered. This quantity represents the average exponential rate of divergence or convergence of nearby orbits in phase space. The general approach for calculating the largest Lyapunov exponent is to follow two nearby orbits and to calculate their average logarithmic rate of separation. Whenever they move too far apart, one of the orbits has to be moved back to the vicinity of the other along the line of separation. For a chaotic attractor, the largest Lyapunov exponent must be positive. If the largest Lyapunov exponent is negative, this implies a stable state or a periodic attractor. The largest Lyapunov exponents of the Ricker mapping have been calculated and plotted in Figure 3. When $0<a<85$, the largest Lyapunov exponent is negative. When $a>85$, the largest Lyapunov exponent is positive. The dynamics behavior is chaotic. And the chaotic attractor is found, as LE max = 22.
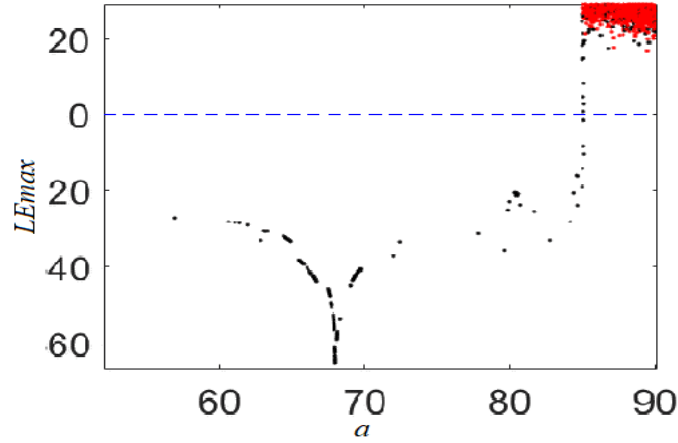

Figure 3: Lyapunov exponents of Ricker mapping ($\gamma = 0.2, \lambda = 0.1, b = 0.2$, $0<a<90$).

4. Pole assignment technique for controlling chaos

The system is first written in the form of a discrete time (Romeiras, Grebogi, Edward, Dayawansa, 1992)

$$Z_{i+1}=F\left(Z_i,a\right), Z_i \in R^2, a \in R \qquad (11)$$

F is sufficiently smooth, a is an externally adjustable real parameter. That is required $\left|a-\overline{a}\right|<\delta$ at some time, and $\overline{a}$ is a rated value. It is assumed that there is a chaotic attractor of Eq. (11) for $a=\overline{a}$. Now the aim is to change the parameters such that the chaotic attractor involves almost all of the initial conditions, so that the dynamic behavior of the system converges to the desired periodic orbit in the attractor. By the OGY method, due to the ergodicity of the chaos dynamics, when the state trajectory enter the vicinity of the unstable periodic orbit to be stabilized, a feedback control law is applied to control the trajectory to move to the desired unstable periodic orbit.

If $Z_*\left(\overline{a}\right)$ is the unstable fixed point, by first-order Taylor expansion, Eq. 11 can be written

$$Z_{i+1} - Z_*(\bar{a}) = A\left(Z_i - Z_*(\bar{a})\right) + B(a - \bar{a}) \tag{12}$$

Find out the values of the matrices A and B at $Z = Z_*(\bar{a})$ and $a=\bar{a}$, where A is the partial

derivative matrix of $F(z, a)$ to z, $A = D_z F(z,a)$ and B is the partial derivative matrix of $F(z, a)$

to a, $B = D_a F(z,a)$. The time dependent control parameter a is in the form of a linear function

with respect to the variable,

$$a - \bar{a} = -K^T\left(Z_i - Z_*(\bar{a})\right) \tag{13}$$

Replace Eq. (13) into Eq. (12)

$$Z_{i+1} - Z_*(\bar{a}) = \left(A - BK^T\right)\left(Z_i - Z_*(\bar{a})\right) \tag{14}$$

So as long as the matrix $A - BK^T$ is asymptotically stable, that is, if the modulus of its

eigenvalues is less than 1, the fixed point $Z_*(\bar{a})$ is stable. The following key questions is how

to determine the matrix K^T, which can stabilize the chaotic motion at a stable periodic point. The

pole assignment is solved according (Ogata, 1990). The matrix $C_{n\times n}$ is controllable matrix, and

the rank is n.

$$C = \begin{pmatrix} B & AB & A^2B \cdots A^{n-1}B \end{pmatrix} \tag{15}$$

The solution of pole assignment is given out by $K^T = \left(\alpha_n - a_n, \cdots, \alpha_1 - a_1\right)T^{-1}$, where

$T = CW$, W is a matrix of order n.

$$W = \begin{pmatrix} a_{n-1} & a_{n-2} & \dots & a_1 & 1 \\ a_{n-2} & a_{n-3} & \dots & 1 & 0 \\ \dots & \dots & \dots & \dots & \dots \\ a_1 & 1 & \dots & 0 & 0 \\ 1 & 0 & \dots & 0 & 0 \end{pmatrix} \tag{16}$$

$a_i \ (i = 1,...,n)$ are the coefficients of the characteristic polynomial of the matrix A,

$$\det(\lambda I - A) = \lambda^n + a_1\lambda^{n-1} + \cdots + a_n \tag{17}$$

And $\alpha_1, \alpha_2, \dots \alpha_n$ are the coefficients of the characteristic polynomial of the characteristic

polynomial $\det(A - BK^T)$,

$$\det\left(sI - \left(A - BK^T\right)\right) = s^n + \alpha_1 s^{n-1} + \cdots + \alpha_n \tag{18}$$

After working out K^T, $\left|K^T\left(Z_i - Z_*(\bar{a})\right)\right| < \delta$ is obtained by $\left|a - \bar{a}\right| < \delta$ and Eq. (14).

5. The chaos control of Ricker mapping

As shown in Figure 4, at $\gamma = 0.2, \lambda = 0.1, b = 0.2$, when $a = 85$, the dynamic has period-1

point and period-2 points. The dynamic behavior of the mapping is chaotic at $\overline{a}=85$. At the same time, there is a strange attractor, which is the closure of the unstability manifolds of the saddle points. And there is an infinite number of unstable periodic orbits in the strange attractor. There are an unstable fixed point $(x_*, y_*) = (57.07, 8.256)$ and the points with period-2 $(x_1, y_1) = (63.725, 6.03)$, $(x_2, y_2) = (101.52, 4.57)$ embedded in the strange attractor.
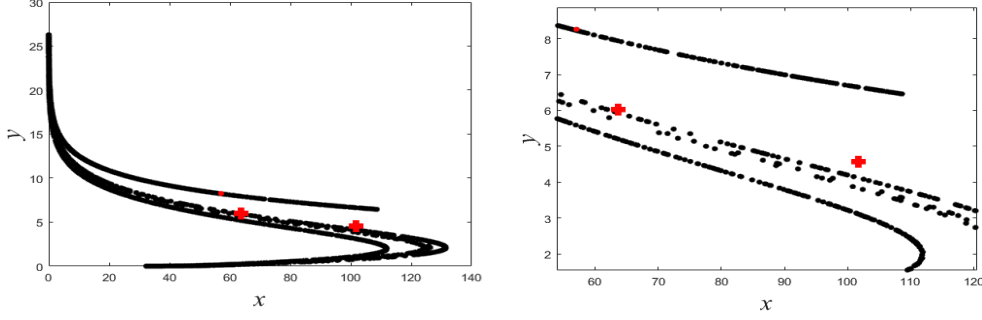

Figure 4: The strange attractor of the Ricker mapping with

unstable periodic orbits of period-1(.) and period-2(+).

5.1. Control of period-1 point of Ricker mapping

Let the control parameter a be a variable near the rated value $\overline{a}=85$, at $\gamma = 0.2, , b = 0.2$, $\lambda = 0.1$, then the matrixes A and B have the following results.

$$A = \left.\left(\begin{array}{cc} (a - \lambda ax - \lambda\gamma ay)\mathrm{e}^{-\lambda(x+y)} & (\gamma a - \lambda ax - \lambda\gamma ay)\mathrm{e}^{-\lambda(x+y)} \\ b & 0 \end{array} \right) \right|_{(x_*, y_*) = (57.07, 8.256)}$$

$$= \left(\begin{array}{cc} -2.7734 & -3.5426 \\ 0.2 & 0 \end{array} \right) \tag{15}$$

$$B = \left.\left(\begin{array}{c} (x + y)\mathrm{e}^{-\lambda(x+y)} \\ 0 \end{array} \right) \right|_{(x_*, y_*) = (57.07, 8.256)} = \left(\begin{array}{c} 0.4394 \\ 0 \end{array} \right) \tag{16}$$

A controllable matrix is a matrix with rank 2 as

$$C = (B \quad AB) = \left(\begin{array}{cc} 0.4394 & -1.2186 \\ 0 & 0.0879 \end{array} \right) \tag{17}$$

The solution of the pole assignment problem is given by $K^{\mathrm{T}} = (\alpha_2 - a_2, \alpha_1 - a_1)T^{-1}$, where

$$T = CW, W = \begin{pmatrix} a_1 & 1 \\ 1 & 0 \end{pmatrix}.$$ a_i $(i = 1, 2)$ are the coefficients of the characteristic polynomial of

the matrix A.

$$\det(\lambda I - A) = \det\begin{pmatrix} \lambda + 2.7734 & 3.5426 \\ -0.2 & \lambda \end{pmatrix} = \lambda^2 + 2.7734\lambda + 0.7085 \qquad (18)$$

So $a_1 = 2.7734, a_2 = 0.7085$.

$$T = CW = \begin{pmatrix} 0.4394 & -1.2186 \\ 0 & 0.0879 \end{pmatrix}\begin{pmatrix} 2.7734 & 1 \\ 1 & 0 \end{pmatrix} = \begin{pmatrix} 2.1612 & 0.4394 \\ 0.0879 & 0 \end{pmatrix} \qquad (19)$$

thus

$$T^{-1} = \begin{pmatrix} 0 & 11.3766 \\ 2.2758 & -55.9559 \end{pmatrix} \qquad (20)$$

The characteristic roots of A which can also be obtained at the fixed point $(x_*, y_*) = (57.07, 8.256)$ are $\lambda_s = -0.2847, \lambda_u = -2.4887$. α_1, α_2 are the coefficients of the characteristic polynomial of the matrix $A - BK^T$. The assumed characteristic roots μ_1, μ_2 are called the adjustment values, that is

$$\det(sI - (A - BK^T)) = s^2 - (\mu_1 + \mu_2)s + \mu_1\mu_2 \qquad (21)$$

The relationships between the roots and the coefficients are obtained as

$$\alpha_1 = -(\mu_1 + \mu_2), \alpha_2 = \mu_1\mu_2 \qquad (22)$$

When $\mu_1 = 1$, $\alpha_1 = -1 - \alpha_2$; when $\mu_1 = -1$, $\alpha_1 = 1 + \alpha_2$ and when $\mu_1\mu_2 = 1$, $\alpha_2 = 1$. According to

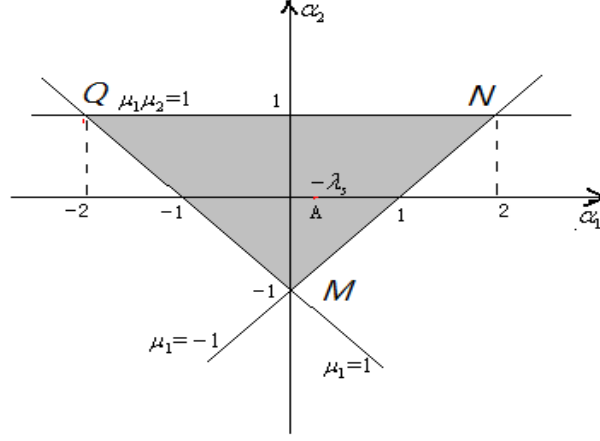the range of the values α_1, α_2 determined above, as in the shaded area in Figure 5.

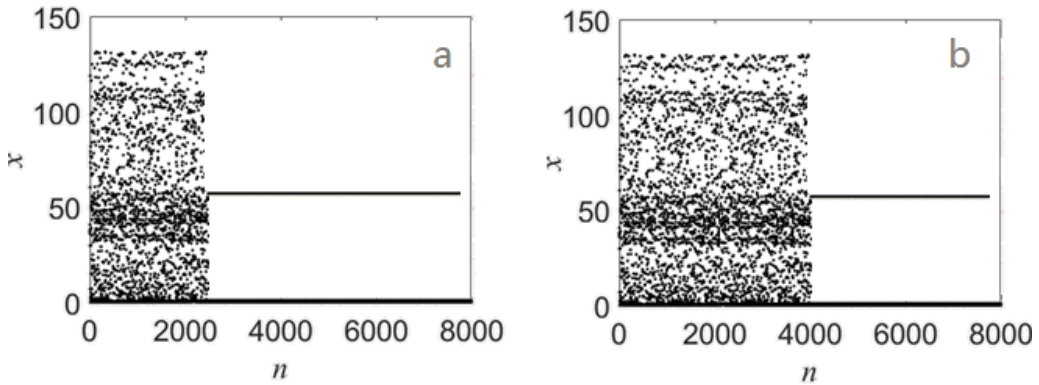Figure 5: Choice of regulator poles area (Triangle region MNQ).

From the previous introduction, we know the matrix K^T is not unique. As long as the matrix K^T is obtained with the values α_1, α_2 in the triangle region as Figure 5, then it can make the matrix $A - BK^T$ be asymptotically stable, that is, the modulus of its eigenvalues is less than 1, so we can take $\mu_1 = 0, \mu_2 = \lambda_s$. As $(\alpha_1, \alpha_2) = (-\lambda_s, 0)$, we can obtain

$$K^T = (0 - a_2, -\lambda_s - a_1) T^{-1} = (-5.6638, 147.3177) \tag{23}$$

When K^T is found, $\left| K^T (Z_i - Z_*(\overline{a})) \right| < \delta$ is obtained by $|a - \overline{a}| < \delta$ and Eq. (14). Thus there is a region whose width is $2\delta / |K^T|$, when Z_i in this region, the parameter is controlled, otherwise the parameter is not controlled. The control rate is given by the following formula

$$a - \overline{a} = -K^T (Z_i - Z_*(\overline{a})) \times u\left(\delta - \left| K^T (Z_i - Z_*(\overline{a})) \right| \right) \tag{24}$$

where u is a step function: $u(\alpha) = \begin{cases} 0, & \alpha < 0 \\ 1, & \alpha > 0 \end{cases}$.
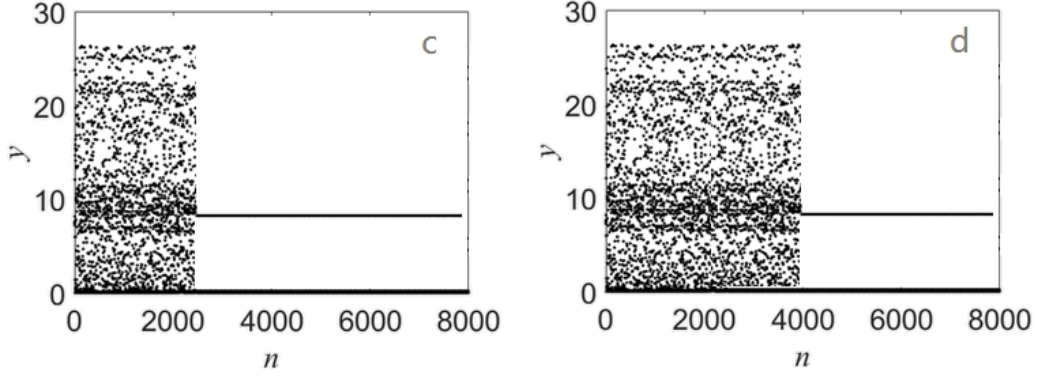
Figure 6:　Control of period-1 of Ricker mapping.

As shown in Figure 6, when we choose $\alpha_1 = 2.7734, \alpha_2 = 0.7085$ in the triangle region of Figure 5, the chaotic motion can be controlled on the period-1 orbit at n=2430 (as shown in Figure 6 a, c). When we choose $\alpha_1 = -0.5, \alpha_2 = 1$, the chaotic motion can be controlled on the period-1 orbit at n=4130 (as shown in Figure 6 b, d). The different value makes the control time different, the number of the Eq. (10) iterations is different to control chaos.

5.2. Control of period-2 of Ricker mapping

By iterating the Eq. (10), we can obtain

$$R\left(R_{a,b}\left(x,y\right)\right):\begin{cases}F\left(x,y,a\right)\\G\left(x,y,a\right)\end{cases} \tag{25}$$

where

$$F\left(x,y,a\right)=\left(a^2\left(x+\gamma y\right)\left(1+x+y\right)^{-\beta}+\gamma ay\right)\left(1+\left(ax+\gamma ay\right)\left(1+x+y\right)^{-\beta}+y\right)^{-\beta} \tag{26}$$
$$G\left(x,y,a\right)=b^2 x$$

When $\bar{a}$=85 , the points $\left(x_1,y_1\right)$ and $\left(x_2,y_2\right)$ of the period two are (63.725,6.03), (101.52,4.57), which are obtained as follows $F\left(x,y,a\right)=x , G\left(x,y,a\right)=y$.

According to

$$A_1 = \begin{pmatrix}\partial F\left(x,y,a\right)/\partial x & \partial F\left(x,y,a\right)/\partial y\\\partial G\left(x,y,a\right)/\partial x & \partial G\left(x,y,a\right)/\partial y\end{pmatrix}_{\left(x_1,y_1\right)} \tag{27}$$

$$A_2 = \begin{pmatrix}\partial F\left(x,y,a\right)/\partial x & \partial F\left(x,y,a\right)/\partial y\\\partial G\left(x,y,a\right)/\partial x & \partial G\left(x,y,a\right)/\partial y\end{pmatrix}_{\left(x_2,y_2\right)} \tag{28}$$

and

$$B_1 = \begin{pmatrix}\partial F\left(x,y,a\right)/\partial a\\\partial G\left(x,y,a\right)/\partial a\end{pmatrix}_{\left(x_1,y_1\right)} \tag{29}$$

11

$$B_2 = \left. \begin{pmatrix} \partial F(x,y,a)/\partial a \\ \partial G(x,y,a)/\partial a \end{pmatrix} \right|_{(x_2,y_2)} \tag{30}$$

Where

$$\partial F(x,y,a)/\partial x = \left(a^2 - \lambda a^2 x - \lambda a^2 \gamma y + \left(\lambda a^2 x + \lambda a^2 \gamma y - \lambda a\right)\right)$$

$$\left(\left(a^2 x + a^2 \gamma y\right)e^{-\lambda(x+y)} + a\gamma y\right)\right)e^{-\lambda\left((ax+\gamma ay)e^{-\lambda(x+y)} + y\right)}e^{-\lambda(x+y)} \tag{31}$$

$$\partial F(x,y,a)/\partial y = \left(\left(a^2\gamma - \lambda a^2 x - \lambda a^2 \gamma y\right)e^{-\lambda(x+y)} + a\gamma + \left(\left(\lambda^2 ax + \lambda^2 a\gamma y - a\lambda\gamma\right)e^{-\lambda(x+y)} - \lambda\right)\right)$$

$$\left(\left(a^2 x + a^2 \gamma y\right)e^{-\lambda(x+y)} + a\gamma y\right)\right)e^{-\lambda\left((ax+\gamma ay)e^{-\lambda(x+y)} + y\right)} \tag{32}$$

$$\partial G(x,y,a)/\partial x = b^2, \quad \partial G(x,y,a)/\partial y = 0 \tag{33}$$

$$\partial F(x,y,a)/\partial a = \left(\left(2ax + 2a\gamma y\right)e^{-\lambda(x+y)} + \gamma y - \left(\lambda x + \lambda\gamma y\right)e^{-\lambda(x+y)}\right)$$

$$\left(\left(a^2 x + a^2 \gamma y\right)e^{-\lambda(x+y)} + a\gamma y\right)\right)e^{-\lambda\left((ax+\gamma ay)e^{-\lambda(x+y)} + y\right)} \tag{34}$$

$$\partial G(x,y,a)/\partial a = 0 \tag{35}$$

Bring $(x_1, y_1) = (63.725, 6.03)$ and $(x_2, y_2) = (101.52, 4.57)$ into the Eq. (34-38).

$$A_1 = \begin{pmatrix} -2.54 & -2.98 \\ 0 & -4.23 \end{pmatrix}, A_2 = \begin{pmatrix} 0.065 & 0.98 \\ 0 & -3.27 \end{pmatrix} \tag{36}$$

$$B_1 = \begin{pmatrix} 0 \\ 0.45 \end{pmatrix}, \quad B_2 = \begin{pmatrix} 0 \\ -0.72 \end{pmatrix} \tag{37}$$

Thus the controllable matrices are obtained as following

$$C_1 = \begin{pmatrix} B_1 & A_1 B_1 \end{pmatrix} = \begin{pmatrix} 0 & -1.34 \\ 0.45 & -1.90 \end{pmatrix} \tag{38}$$

$$C_2 = \begin{pmatrix} B_2 & A_2 B_2 \end{pmatrix} = \begin{pmatrix} 0 & 0.44 \\ -0.72 & 6.23 \end{pmatrix} \tag{39}$$

$a_i \ (i=1,2)$ are the coefficients of the characteristic polynomial of the matrix A_1, $a_1 = 4.23, a_2 = 10.74$, At the same time, the characteristic roots are $\lambda_{1s} = -0.58$, $\lambda_{1u} = -4.45$. The solution of the pole assignment problem is given by

$$K_1^{\mathrm{T}} = \left(\alpha_2 - a_2, \alpha_1 - a_1\right) T_1^{-1} \tag{40}$$

α_1, α_2 are the coefficients of the characteristic polynomial of the matrix $A_1 - B_1 K_1^{\mathrm{T}}$, According

to the discussion of the values α_1, α_2, we still take $(\alpha_1, \alpha_2) = (-\lambda_{1s}, 0)$, where $T_1 = C_1 W_1$, so

$$K_1^{\mathrm{T}} = (0 - a_2, -\lambda_{1s} - a_1) T_1^{-1} = (-4.1420, -4.3561) \tag{41}$$

$a_i (i = 3, 4)$ are the coefficients of the characteristic polynomial of the matrix $A_2 - B_2 K_2^{\mathrm{T}}$,

$a_3 = 2.65, a_4 = -0.15$, the characteristic roots is $\lambda_{2s} = 0.043, \lambda_{2u} = -4.12$. We take

$(\alpha_3, \alpha_4) = (-\lambda_{2s}, 0)$, thus we obtain $K_2^{\mathrm{T}} = (-0.3947, 6.1640)$. The control rate can be given

by the following equation.

$$a - \bar{a} = -K_i^{\mathrm{T}} \left(Z_n - Z(i)(\bar{a}) \right) \times u \left(\delta - \left| K_i^{\mathrm{T}} \left(Z_n - Z(i)(\bar{a}) \right) \right| \right), (i = 1, 2) \tag{42}$$
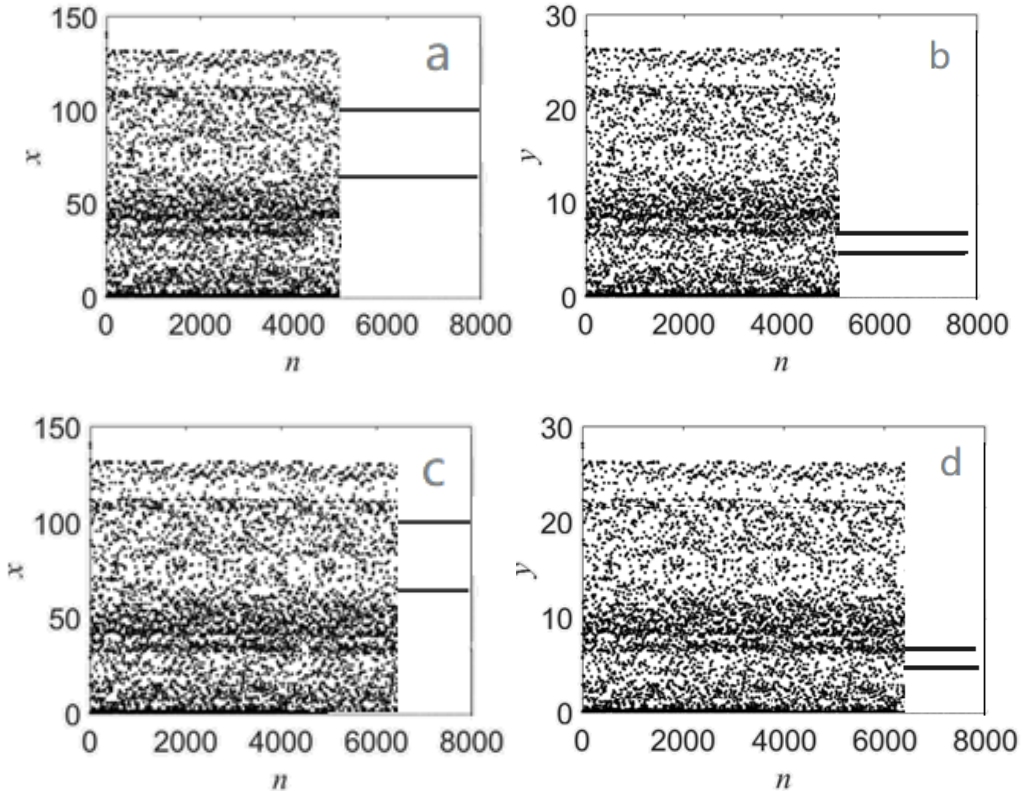

Figure 7: Control of period-2 of Ricker mapping.

As shown in Figure 7, when we choose $\alpha_1 = -0.47, \alpha_2 = 0, \alpha_3 = -0.28, \alpha_4 = 0$ in the

triangle region of Figure 5, the chaotic motion can be controlled on the period-2 orbits at $n=5080$

(as shown in Figure 7. a, b). When we choose $\alpha_1 = -0.3, \alpha_2 = 0.2, \alpha_3 = -0.25, \alpha_4 = -0.54$,

the chaotic motion can be controlled on the period-2 orbits at $n=6350$ (as shown in Figure 7. c, d).

6. Conclusion

The dynamic behavior of the Ricker mapping is very complex in different values of a. When

13

the value of *a* is changed from 0.455 to 90, the mapping goes through doubling bifurcation to Hopf bifurcation. Several strange attractors coexist at last. Through the numerical simulation and analysis of the bifurcation and phase diagrams of the mapping, it is consistent with the theoretical analysis. By improving the method of the OGY, the chaotic control of the Ricker mapping is controlled, the perturbation quantity of the control parameter is selected by the pole configuration method in the linear control theory, the unstable period-1 and the unstable period-2 are controlled to be stable period orbits. At the same time, the adjustment values to be selected are different, the number of the mapping iterations is different to control chaos. By numerical simulation, the effectiveness of the method is demonstrated．According to the research results, the birth rate *a*, survival rate *b* or decay coefficient *γ* can be properly adjusted to achieve an ecological balance. The analysis and results in this paper are interesting in mathematics and biology.

Data Accessibility Statement：No data, models, or code were generated or used during the study.

References

[1]Caswell H. (2001). *Matrix Population Models*. 2nd edn (Sunderland, MA: Sinauer).

[2]Ilie Ugarcovici and Weiss H. (2007). Strange attractors and physical measures for some density dependent Leslie population models. *Nonlinearity*, *720*: 2897-2906.

[3]IIie Ugarcovici and Weiss H. (2004). Chaotic dynamics of a nonlinear density dependent population model. *Nonlinearity*, *17*: 1689-712.

[4]Wikan A. and Mjølhus E. (1996). Over compensatory recruitment and generation delay in discrete age-structured population models. *J. Math. Biol.*, *35*: 195-239.

[5]Ott E., Grebogi C., Yorke J. A. (1990). Controlling chaos. *Phys. Rev Lett*, *64*(11):1196-1199.

[6]Pyragas K. (1992). Continuous control of chaos by self-controlling feedback. *Phys. Lett A*, *170*: 421-428.

[7]Shinbrot T., Grebogi C., Ott E. (1993). Using small perturbations to control chaos. *Nature*: (London), *363*: 411-417.

[8]Pyragas K. (1993). Predictable chaos in slightly perturbed unpredictable chaotic systems. *Phys. Lett A*, *181*: 203-210.

[9]Kocarev L., Parlitz U. (1995). General approach for chaotic synchronization with applications to communication. *Phys. Rev Lett*, *74*: 5028-5031.

[10] Atike Reza Ahrabi (2019). A chaos to chaos control approach for controlling the chaotic dynamical systems using Hamilton energy feedback and fuzzy-logic system. *Chaos*, *4*(1): 1056-1069.

[11] El-Sayed A. M. A., Elsaid A., Nour H. M., Elsonbaty A. (2013). Dynamical behavior, chaos control and synchronization of a memristor-based ADVP circuit. *Communications in Nonlinear Science and Numerical Simulation*, *18*(1): 148-170.

[12] Sanju Saini (2015). GA optimized time delayed feedback control of chaos in a memristor based chaotic circuit. *IEEE symposium on computational intelligence*, *23*(3): 198-210.

[13] Herbert Ho-Ching Iu, Andrew L Fitch (2013). Controlling chaos in a memristor based circuit. *Development of Memristor Based Circuits*, *34*: 13-36.

[14] Hassan Saberi Nik, Sohrab Effati (2014). JAFAR Saberiadjafi. Ultimate bound sets of a hyper chaotic system and its application in chaos synchronization. *Complexity*, *20*(4):456-476.

[15] Wu T., Chen M. S. (2008). Chaos control for chua's circuits. *Control of Chaos in Nonlinear Circuits and Systems*, *23*: 97-164.

[16] Xian Liu, Lin Huang (2006). Chaos control of a four order chua's circuit. *Control Conference*, *24*(5): 567-589.

[17] Guo Feng (2018). The dynamic property and chaos control for a two-degree-of-freedom vibro-impact system. *U.P.B. Sci. Bull., Series D*, *80*(1): 1454-2358.

[18] Flipe J. Romeiras, Grebogi C., Edward Ott, Dayawansa W. P. (1992). Controlling chaotic dynamical systems. *Phys. D*, *58*:165-192.

[19] Leslie P. (1945). On the use of matrices in population mathematics. *Bio. metrika*, *33*:183-212.

[20] Leslie P. (1948). Some further notes on the use of matrices in population mathematics. *Bio. Metrika*, *35*: 213-245.

[21] Quinn T. and Deriso R. (1999). *Quantitative fish dynamics* (Oxford: Oxford University Press).

[22] Ogata K. (1990).*Controlling engineering*. Second Ed. (Prentice Hall, Englewood Cliffs, NJ, 782-784.